Chaos

Deconfinement of classical Yang–Mills color fields in a disorder potential

Cite as: Chaos **31**, 093106 (2021); https://doi.org/10.1063/5.0057969
Submitted: 26 May 2021 . Accepted: 20 August 2021 . Published Online: 08 September 2021

Leonardo Ermann, and Dima L. Shepelyansky

Deconfinement of classical Yang–Mills color fields in a disorder potential

Cite as: Chaos **31**, 093106 (2021); doi: 10.1063/5.0057969
Submitted: 26 May 2021 · Accepted: 20 August 2021 ·
Published Online: 8 September 2021

Leonardo Ermann[1,2] and Dima L. Shepelyansky[3,a)]

AFFILIATIONS

[1]Departamento de Física Teórica, GIyA, Comisión Nacional de Energía Atómica, 1429 Buenos Aires, Argentina
[2]Consejo Nacional de Investigaciones Científicas y Técnicas (CONICET), C1425FQB Buenos Aires, Argentina
[3]Laboratoire de Physique Théorique, Université de Toulouse, CNRS, UPS, 31062 Toulouse, France

[a)]**Author to whom correspondence should be addressed:** dima@irsamc.ups-tlse.fr

ABSTRACT

We study numerically and analytically the behavior of classical Yang–Mills color fields in a random one-dimensional potential described by the Anderson model with disorder. Above a certain threshold, the nonlinear interactions of Yang–Mills fields lead to chaos and deconfinement of color wavepackets with their subdiffusive spreading in space. The algebraic exponent of the second moment growth in time is found to be in the range of 0.3–0.4. Below the threshold, color wavepackets remain confined even if a very slow spreading at very long times is not excluded due to subtle nonlinear effects and the Arnold diffusion for the case when initially color packets are located in close vicinity. In the case of large initial separation of color wavepackets, they remain well confined and localized in space. We also present the comparison with the behavior of the one-component field model of discrete Anderson nonlinear Schrödinger equation with disorder.

The spacial dynamics of classical Yang–Mills color fields in a disorder potential is investigated. The nonlinear interactions of colors are characterized by a certain interaction constant. It is shown that for the constant being above a chaos threshold, there is a deconfinement of color packets with a subdiffusive spreading in space. Below the threshold, color wavepackets remain confined in space for extremely large times. For initially separated color packets, the interactions drop exponentially with the separation so that the packets are confined due to the phenomenon of Anderson localization of quantum waves in a disorder potential. It is argued that this system captures generic features of interacting nonlinear oscillators with disordered frequencies distributed in space.

I. INTRODUCTION

Yang–Mills (YM) gauge fields were introduced[1] for an isotropic-invariant description of strong interactions. The investigation of properties of these fields still remains an interesting and important problem. The studies of classical YM fields are also important for applications in solving several problems of quantization.[2,3] The classical dynamics of these fields is essentially nonlinear and nontrivial. Its analysis is rather important for semiclassical description of strong YM vacuum fluctuations.[4–7] Thus, the investigation of nonlinear dynamics and time evolution of classical YM fields represents a relevant topic.

An important class of classical YM models was introduced in Ref. 8, where the YM fields are homogeneous in space so that the time evolution is described only by nonlinear dynamics of interacting colors. In general, this Hamiltonian dynamics of color YM fields was shown to be chaotic[9–11] even if certain integrable solutions also exist. Thus, the YM dynamics belongs to a generic class of chaotic Hamiltonian systems with divided phase space with small integrability islands embedded in a chaotic sea.[13,14] Even if important mathematical results have been obtained for chaotic dynamics (see, e.g., Refs. 15 and 16), the properties of chaos with such a divided phase space, composed of integrable islands surrounded by a chaotic component, still remain very difficult for mathematical analysis. The existence of chaos of classical homogeneous YM fields has been reported already some time ago,[8–11] but still these YM fields and related models attract the attention of researchers (see, e.g., Refs. 17–19).

The above dynamics of YM color fields can be reduced to a rather simple Hamiltonian, for which $N_C = 2, 3$

colors reads

$$H = \sum_{\mu=1}^{N_C} (p_\mu{}^2 + m x_\mu{}^2)/2 + \beta \sum_{\mu' \neq \mu} x_{\mu'}{}^2 x_\mu{}^2/2, \quad (1)$$

where (p_μ, x_μ) are the effective conjugated momentum and coordinate, color index is $\mu = 1, \ldots, N_C$, m is the mass, which is zero or finite in the presence of Higgs mechanism, and β determines the strength of nonlinear interactions of colors. The derivation of these models and their properties are described in detail in Refs. 8–12. An interesting feature of the finite mass case (e.g., $m = 1$ in dimensionless units used here) is that the measure of chaos remains finite and large (about 50%) even in the limit of very weak nonlinearity $\beta \to 0$ since the Kolmogorov–Arnold–Moser (KAM) theorem[14] is not valid when all color masses (or oscillator frequencies) are the same.[11]

To date, the classical dynamics of YM colors was analyzed for fields that are homogeneous in space. Here, we consider the case of space nonhomogeneous fields. In particular, we study the spreading of such YM fields in space in the presence of random (or disorder) potential, which corresponds to another generic limiting case of space properties. Such a disorder corresponds to random properties of vacuum in Quantum Chromodynamics (QCD) discussed in Refs. 20–23. It is well known that in quantum mechanics, a random potential may lead to a localization of probability spreading due to quantum interference effects. This phenomenon is known as the Anderson localization[24] and plays an important role for electron transport in solid-state systems with disorder.[25–27] The eigenstates of such a system are exponentially localized in one and two dimensions (1D and 2D) while in three dimensions (3D), a delocalization transition takes place at a disorder below a certain threshold (see, e.g., the review of Ref. 27).

The effects of nonlinearity on Anderson localization in 1D lattice were investigated in Ref. 28, where it was shown that the localization is preserved at weak nonlinearity while above a certain threshold, a subdiffusive spreading over the whole lattice takes place. The detailed numerical studies of this phenomenon in Disordered Anderson Nonlinear Schrödinger Equation (DANSE) have been reported in Refs. 29–32, and the results of different groups were reviewed in Refs. 33 and 34. The subdiffusive spreading has been studied for various nonlinear models in 1D and 2D (see, e.g., Refs. 35–39). Thus, spreading continuing up to enormously long times $t \sim 2 \times 10^{12}$ (expressed in map iterations) was reported for a 1D nonlinear map model.[38] The interest of nonlinear effects for Anderson localization is also supported by related experimental studies of wave propagation in disordered nonlinear media[40,41] and spreading of Bose–Einstein cold atom condensates in optical lattices[42,43] described by the Gross–Pitaevskii equation.

All of the above investigations of packet spreading in a random potential with nonlinearity have been done for one-component nonlinear field of DANSE with nonlinear self-interaction (see, e.g., Ref. 30, 33, and 34). The case of YM color dynamics is different since nonlinearity appears only due to interactions of color components. In fact, possible implications of randomness, dynamical chaos, Anderson localization, and confinement have been discussed in Refs. 21 and 22. The deconfinement transition in QCD at finite temperature is also under active investigation (see, e.g., Refs. 44–46, and references therein). Here, we find that under certain conditions, the nonlinear interaction of YM colors leads to deconfinement of YM fields and their unlimited subdiffusive spreading in space. In the case of weak nonlinearity or spacial separation of YM color components, the Anderson localization is preserved and color fields remain localized in space. We hope that the obtained results may be of interest for the deconfinement phenomenon of quantum YM fields, which attracts significant interest.

This paper is organized as follows: in Sec. II, we give the system description; the numerical and analytical results are given in Sec. III; and discussion of results is given in Sec. IV.

II. MODEL DESCRIPTION

A. DANSE

We start with a brief description of the DANSE model studied in Refs. 30 and 33–35. The wavefunction evolution of DANSE is described by the equation

$$i\hbar \frac{\partial \psi_n}{\partial t} = E_n \psi_n + \beta |\psi_n|^2 \psi_n + V(\psi_{n+1} + \psi_{n-1}). \quad (2)$$

Here, β determines nonlinearity strength, V gives near-neighboring hopping matrix element, on-site disorder energies are randomly distributed in the range $-W/2 < E_n < W/2$, and the total probability is conserved and normalized to unity $\sum_n |\psi_n|^2 = 1$. Thus, W determines the strength of disorder. For $\beta = 0$, all eigenstates are exponentially localized with $|\psi| \propto \exp(-|n - n_0|/\ell)$ and localization length is $\ell \approx 96(V/W)^2$ at the energy band center and weak disorder.[47] Here, n_0 marks a center of wavefunction. We consider a case of relatively weak disorder with $\ell > 1$. For convenience, we set $\hbar = V = 1$ so that the energy coincides with the frequency.

Above a certain threshold $\beta > \beta_c$, the nonlinearity leads to a destruction of localization with a subdiffusive spreading of wavepacket width $\Delta n = n - n_0$,

$$\sigma = \langle (\Delta n)^2 \rangle \propto t^\alpha, \quad (3)$$

where brackets mark averaging over wavefunction at time t and α is the subdiffusion exponent. The numerical simulations give its value being in the range of $0.3 \leq \alpha \leq 0.4$. Certain analytical arguments were given for values $\alpha = 0.4$[28,30,35] and $\alpha = 1/3$ (see Ref. 32, review of Ref. 34, and references therein). An introduction of randomness in eigenstate phases of linear problem produces spreading with $\alpha = 0.5$ (see Refs. 34 and 48, and references therein). Indeed, an increase of dephasing, modeled by an increase of number of driving frequencies, leads to a growth of α approaching the value $\alpha = 0.5$.[37]

It is difficult to give an exact estimate of the threshold value β_c. The numerical results show that at $\beta = 0.1, 0.03$, the wavepacket square width σ remains bounded without a significant increase up to times $t = 10^8$.[30] However, it is possible that some type of Arnold diffusion along tiny chaotic layers[13,14,49] may lead to a very slow spreading of a very small wavepacket fraction. It should be pointed that the Anderson localization is characterized by a pure-point dense spectrum and its perturbation by nonlinearity represents a very difficult problem for mathematical analysis. A reader can find some mathematical results for this problem reported in Refs. 50 and 51.

A surprising feature of unlimited spreading at $\beta > \beta_c$ is that with growth of Δn, the relative local contribution of nonlinear term in (2) decreases as $\beta|\psi|^2 \sim \beta/\Delta n \propto \beta/t^{\alpha/2}$ and on a first

glance, it seems that nonlinearity becomes weaker and weaker with time. In Ref. 28, it was argued that even being small this term gives a local nonlinear frequency spreading $\delta\omega \sim \beta/\Delta n$, which at $\beta > \beta_c \sim 1$ remains larger than the typical spacing $\Delta\omega \sim 1/\Delta n$ between frequencies of linear eigenmodes populated due to subdiffusive spreading of wavepacket at time t. As soon as $\delta\omega > \Delta\omega$, the spectrum of motion remains continuous and thus the spreading can continue unlimitedly in time. However, a better understanding of such unlimited spreading is still highly desirable.

B. YM color models

In a similarity with dynamics of homogeneous YM fields described by Hamiltonian (1) and DANSE (2), we model the dynamics of YM color fields in a potential by the nonlinear Schrödinger equation

$$i\frac{\partial \psi_n^\mu}{\partial t} = E_n\psi_n^\mu + \beta\left(\sum_{\mu'\neq\mu} |\psi_n^{\mu'}|^2\right)\psi_n^\mu + (\psi_{n+1}^\mu + \psi_{n-1}^\mu). \quad (4)$$

Here, $\mu = 1, \ldots, N_C$ is the color index changing from 1 to 2 for two YM colors $N_C = 2$ or from 1 to 3 for three colors $N_C = 3$. We denote these two cases as *YMCA*2 and *YMCA*3, respectively (with A for agent and YMCA for Yang–Mills Color Model Agent). At zero nonlinearity $\beta = 0$, each color evolution is described by 1D Anderson model with the same disorder E_n for all colors and being the same as in (2). In the absence of hopping to nearby sites and all energies E_n being equal, we have the dynamics of color fields described by equations similar to those for the homogeneous YM fields from Hamiltonian (1). We do not provide a mathematical derivation of Eq. (4) but we argue that they capture important physical effects: Anderson localization in a random potential for linear waves without color interactions, lattice description of propagation in space often used in QCD lattices, color interactions are the same as for homogeneous YM fields, and a similar lattice description is used in DANSE to model effects of disorder for the Gross–Pitaevskii equation. Thus, we consider Eq. (4) as a realistic model of the evolution of classical YM color fields in a disorder potential.

Here, we consider the cases with only two or three colors studied previously for homogeneous YM fields. In principle, Eq. (4) can also describe a model with four colors by extending the summation over μ index up to $N_C = 4$. This may be useful for investigations of various mathematical models of supersymmetric YM theory (see, e.g., Ref. 52, and references therein).

We discuss some generic properties of YM dynamics (4) in Secs. III and IV. The numerical results are presented in Sec. III.

As for DANSE, the evolution of YM fields (4) has the energy conservation, and also the probability is conserved for each component normalized to unity $\sum_n |\psi_n^\mu|^2 = 1$. The numerical simulations of DANSE and Klein–Gordon nonlinear (KGN) model with disorder (see Refs. 34, 36, and 53, and references therein) show that the exponent α is approximately the same in these two models even if only energy is conserved in the KGN case. Thus, we also expect that the probability conservation for each color component will not affect the spreading exponent α. Indeed, the number of degrees of freedom in (4) is given by the number of lattice sites multiplied by N_C, which is much larger than the number of integrals $N_C + 1$ of energy and component probabilities.

From the structure of YM equation (4), we can make certain direct observations. First, it is possible to consider the symmetric case when initially all color components ψ_n^μ are the same. Then, their evolution is described by the DANSE Eq. (2) with some rescaling of β for $N_C = 3$. However, since the field evolution is chaotic, this solution is unstable and small corrections to this symmetric state grow exponentially with time so that this symmetry is completely destroyed very rapidly. Still such a symmetric case allows us to expect that the spreading exponent α will have a value similar to those found for DANSE. As for DANSE, we expect that YM fields remain confined or localized below a certain chaos threshold with $\beta \ll \beta_c \sim 1$. In spite of this possible similarity between DANSE and YMCA models, there are two important differences between them. Thus, if initially color wavepackets are located far from each other with a typical distance between them, with R_C being significantly larger than the localization length ℓ of the linear case ($R_c \gg \ell$), then an effective interaction between colors becomes exponentially small $\beta_{eff} \propto \beta \exp(-2R_C/\ell)$ so that we have $\beta_{eff} \ll \beta_c \sim 1$. Thus, we expect that such initial states will remain exponentially localized or confined for all times. Another new element of YMCA, compared to DANSE case, is that the eigenenergies ε_m of linear problem eigenmodes at $\beta = 0$ are the same for all colors. Thus, for one site and three colors, we have a dynamics that is very similar to those of Higgs case with finite mass (1) studied in detail in Ref. 11. Due to this degeneracy, the KAM theorem cannot be applied to this system and the measure of chaos remains about 50% even in the limit of nonlinearity going to zero.[11] However, the initial wavepackets of colors should populate the same linear eigenmodes (this requires $R_C < \ell$). Such a situation also generally appears in other nonlinear systems with many degrees of freedom.[54] Since in YMCA at $N_C = 3$ [Eq. (4)], there are many eigenenergies ε_m (linear frequencies) that are the same; we expect that there are many initial configurations when colors are initially located at a distance $R_c \sim \ell$ and their dynamics remains chaotic even for very small nonlinearity $\beta \to 0$. However, a question about the spreading of such chaos over lattice sites remains open.

III. NUMERICAL RESULTS FOR TIME EVOLUTION OF YM COLORS

Following the approach used in Ref. 30, the numerical integration of Eqs. (2) and (4) is done by the Trotter decomposition with a time step $\Delta t = 0.05$ and the total number of sites $N = 1001$ for each color with the fast Fourier transform from coordinate to momentum representation and back. This integration scheme is symplectic and conserves probability exactly. Its efficiency has been confirmed by various numerical simulations (see, e.g., Refs. 30 and 33–35). We checked that the variation of system size N and integration time step Δt does not affect the results. Usually, as in Refs. 30, 33, and 35, we used initial conditions with a population of one or a few nearby sites for each color and energy being in the middle of a linear energy band.

The properties of the above integration scheme had been discussed in detail in Refs. 30, 33, and 35. It exactly preserves the probability thus being symplectic. The energy of the system,

which is also an exact integral of (4), is preserved with an accuracy of 1%. On a first glance, the accuracy seems to be not so high but there is an important physical argument behind, which we illustrate on an example of such an integration scheme (also known as the Euler or Trotter scheme) for pendulum Hamiltonian $H = p^2/2 - \cos x$. Indeed, for a pendulum, this symplectic integration leads to the Chirikov standard map with a chaos parameter $K = (\Delta t)^2 = 2.5 \times 10^{-3}$. From the properties of this map,[13,14] it is known that the main part of the phase space remains integrable with the invariant curves being only slightly deformed compared to the case of the pendulum. The chaos remains only in a tiny chaotic layer around a separatrix of resonances. For the main resonance, its width in frequency is approximately[13] $\delta\omega_s \Delta t = \delta p \Delta t \approx (32\pi^2/K)\exp(-\pi^2/\sqrt{K}) \sim 10^{-80}$, thus being enormously small for $K = (0.05)^2$. We think that this physical argument well justifies the integration scheme used in our simulations here and in Refs. 30, 33, and 35.

We present here the results mainly for a typical disorder strength $W = 4$ and nonlinearity values $\beta = 0, 1, 2, 4$. The spreading of color probabilities is characterized by the squared wavepacket width at different times defined as $\sigma_1 = \langle n_1^2 \rangle - \langle n_1 \rangle^2$ for DANSE, $\sigma_1 = \sum_{\mu=1}^{N_C} \left(\langle n_\mu^2 \rangle - \langle n_\mu \rangle^2 \rangle \right) / N_C$ for YMCA2 and YMCA3, relative square moments $\sigma_2 = \langle (n_1 - n_2)^2 \rangle$ for YMCA2, and $\sigma_2 = \left[\langle (n_1 - n_2)^2 \rangle + \langle (n_1 - n_3)^2 \rangle + \langle (n_2 - n_3)^2 \rangle \right] / 3$ for YMCA3. Here, brackets mark the average over wavefunction. The results are also averaged over 20 disorder realizations.

A. Deconfinement and subdiffusive spreading of YM colors

The time dependence of second moments σ_1 for DANSE and YMCA3 models is shown in Fig. 1 for different values of β and disorder $W = 4$. At such a disorder and $\beta = 0$, the wavepacket spreads on approximately $\Delta n \approx 7$ sites in agreement with the theoretical value of the localization length $\ell = 96/W^2 = 6$. In the presence of nonlinear interactions, there is a subdiffusive spreading of wavepacket, which is somewhat stronger for YMCA3 compared to the DANSE case. The time evolution of the second moment σ_2 for YMCA3 case is shown in Fig. 2 for the same values of β as in Fig. 1. The growth of both moments σ_1 and σ_2 is very similar. This means that the color packets spread in such a way that they remain close to each other so that their effective interactions allow us to make correlated joint transitions over localized eigenstates of the Anderson model at $\beta = 0$. It is clear that interactions of colors lead to deconfinement of YM fields with the unlimited subdiffusive spreading over the whole lattice. The growth of moments σ_1, σ_2 for the YMCA2 case is very similar to those of YMCA3 and we do not show it here (but the obtained exponents α are discussed below for both cases).

In Fig. 3, we show directly the probability distribution over lattice sites $w(n) = \sum_{\mu=1}^{N_C} |\psi_n^\mu|^2 / N_C$ at different moments of time for YMCA3 case with $\beta = 2$. There is a formation of quasi-plateau distribution of size Δn growing with time. Outside of plateau, there are probability tails that drop exponentially with the site number that corresponds to exponentially localized Anderson modes of linear problem.

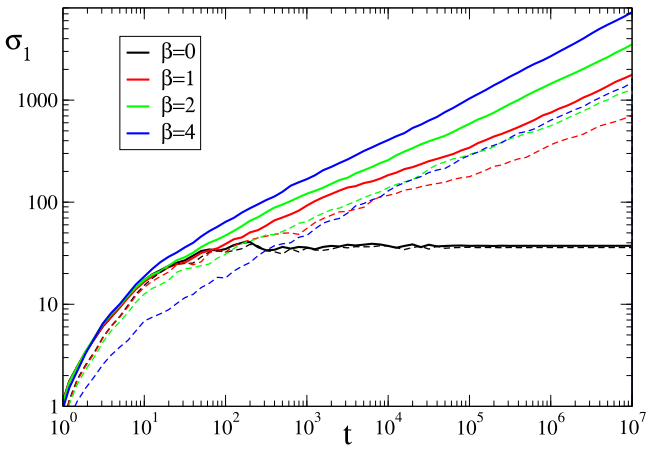

FIG. 1. Time evolution of the second moment σ_1 of the probability distribution, defined in the text, for YMCA3 model with three colors [Eq. (4)] (solid curves) and the DANSE model [Eq. (2)] (dashed curves) at $\beta = 0$ (black curves), $\beta = 1$ (red curves), $\beta = 2$ (green curves), and $\beta = 4$ (blue curves) at $W = 4$. At initial time, the three color packets are located at three different sites at $n = -1, 0, 1$ for YMCA3; for DANSE, the initial probability is at $n = 0$. The average is done over 20 random realizations of disorder and over logarithmic equidistant intervals of time; a typical error bar from these 20 realizations at a given time is $\delta\sigma_1/\sigma_1 = 0.124$ at $t = 10^7$ and $\beta = 4$.

The distributions $w(n)$ at largest reached time $t = 10^7$ and different values of nonlinearity β are shown in Fig. 4. The width of the above quasi-plateau size Δn increases with β being approximately $\Delta n \approx 220, 320, 440$ for $\beta = 1, 2, 4$, respectively (Δn is defined as a size at which an average probability drops by a factor 10 compared to the center). These Δn values are much larger than the Anderson localization length $\ell \approx 6$. Also, the corresponding nonlinear frequency width $\Delta\omega \sim 1/\Delta n \ll 1/\ell$ becomes significantly smaller than a typical frequency spacing between modes inside localization

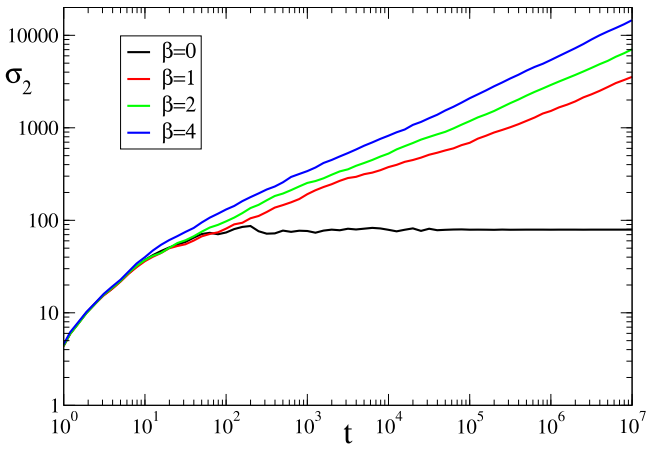

FIG. 2. Same as in Fig. 1 but for the second moment σ_2 of the probability distribution for the YMCA3 model defined in the text.

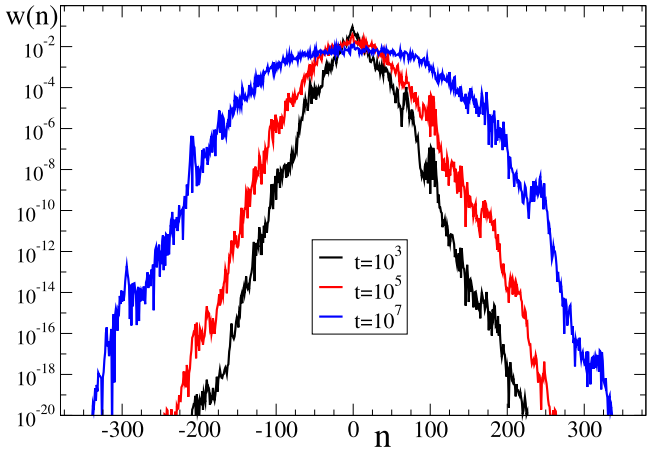

FIG. 3. Probability distributions $w(n) = \sum_{\mu=1}^{N_C} |\psi_n^\mu|^2 / N_C$ for the YMCA3 model ($N_C = 3$, $\beta = 2$, $W = 4$) are shown at times $t = 10^3$ (black curve), $t = 10^5$ (red curve), and $t = 10^7$ (blue curve); probabilities are averaged over 20 disorder realizations.

length ℓ. Due to these reasons, we can argue that the numerical results show an asymptotic spreading of wavepacket of YM colors.

The comparison of probability distributions for DANSE, YMCA2, and YMCA3 models is shown in Fig. 5 for fixed β, W, and $t = 10^7$. The most broad spreading corresponds to YMCA3 case. This is in a qualitative agreement with an expectation that, similar to Hamiltonian (1), there is an exact degeneracy of linear color eigenmodes so that here chaos is present even in the limit of very small β similar to the situation discussed in Refs. 11 and 54 (of course, this assumes that the initial state has a close location of three colors so that degenerate linear modes are well populated; see discussion below).

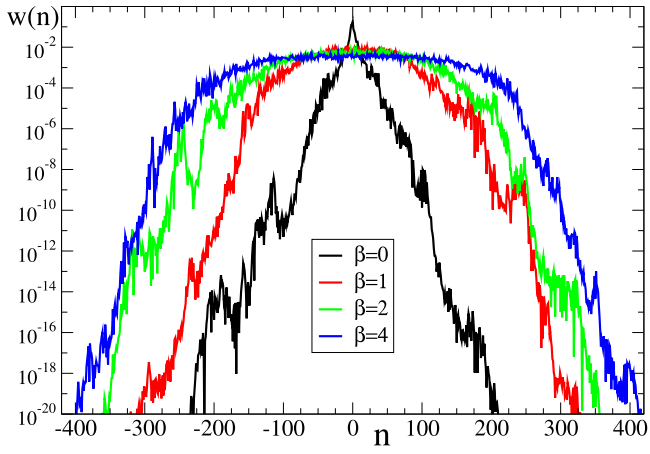

FIG. 4. Same as in Fig. 3 but all distributions $w(n)$ of YMCA3 are shown at time $t = 10^7$ for $\beta = 0$ (black curve), $\beta = 1$ (red curve), $\beta = 2$ (green curve), and $\beta = 4$ (blue curve); probabilities are averaged over 20 disorder realizations.

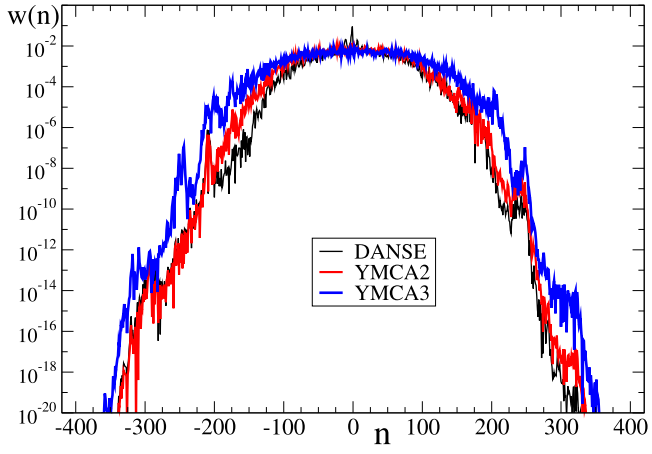

FIG. 5. Probability distributions $w(n)$ are shown for DANSE (black curve), YMCA2 (red curve), and YMCA3 (blue curve) at $\beta = 2$, $W = 4$, and $t = 10^7$; probabilities are averaged over 20 disorder realizations.

According to the results of Figs. 1 and 2, the growth of σ_1, σ_2 at large times is well described by an algebraic function of time with the exponent α. The values of α, obtained from the fit for time range $100 \leq t \leq 10^7$, are given in Table I for DANSE, YMCA2, and YMCA3 models. For DANSE at $\beta = 1$, the obtained value of α is a bit smaller than the one reported in Ref. 30 with $\alpha = 0.306 \pm 0.002$. We attribute this difference to a different number of realizations and the longer time range used in Refs. 30. We also should note that the spreading is rather slow in time and thus very long time simulations and a large number of realizations are required to obtain accurate values of α. Formal statistical errors reported here and in Ref. 30 are relatively small but the contribution of certain systematic effects, related to slow transitions between localized linear modes, may give more significant corrections to formal statistically averaged α values. From Table I, we see a moderate increase of α for higher β values. We also find that YMCA3 and YMCA2 models have a moderately higher values of α compared to DANSE case. We attribute this to a stronger chaos for YM colors compared to DANSE. Indeed, YM colors have additional color degrees of freedom that are supposed to generate a stronger chaos, thus facilitating deconfinement and spreading of YM fields. However, due to the above points related to a slow spreading process, further more advanced studies are required to firmly state if α is independent, or not, of β, W, and the number of colors N_C.

We also did other checks by using another independent sets of random realizations for specific parameter values (e.g., $\beta = 2$ and 3 colors). Thus, as an example, for such a set, the fit of the subdiffusive speading of σ_1 for the same time range $100 < t \leq 10^7$ gives the exponent $\alpha = 0.361 \pm 0.010$, which is well in agreement with the corresponding value in Table I. This gives a confirmation that α values are statistically reliable in a given time range.

B. Confinement and localization of YM colors

Above, we discussed the cases with moderate strength of interactions of colors given by β. It is natural to expect that at

TABLE I. Exponent α of growth of second moments $\sigma_{1,2} \propto t^{\alpha}$ for DANSE, YMCA2, and YMCA3 models at different values of nonlinearity β at $W = 4$; the values of exponent are obtained by a fit in the time interval $2 \leq \log_{10} t \leq 7$ for data averaged over 20 disorder realizations; initial states have colors located close to each other with $R_C = 1$.

	α		
β	DANSE	YMCA2	YMCA3
1	0.26 ± 0.02	0.297 ± 0.020	0.316 ± 0.010
2	0.317 ± 0.010	0.327 ± 0.020	0.363 ± 0.010
4	0.371 ± 0.020	0.378 ± 0.020	0.406 ± 0.010

small $\beta \ll \beta_c \sim 1$ Anderson localization is preserved and fields remain localized in space. Indeed, the numerical results reported for DANSE[30] indicate that localization is preserved at small $\beta = 0.1, 0.03$. At the same time, we note that in this limit, the effects of slow processes like Arnold diffusion[13,49] are still possible with a very slow spreading of a very small fraction of probability via tiny chaotic layers. The mathematical results are not able to clarify the behavior in this regime (see, e.g., Refs. 50 and 51).

For the YMCA3 case, at such small values of nonlinearity $\beta = 0.1, 0.03$, we show the time dependence of the second moment σ_1 in Fig. 6. Here, the second moment σ_1 remains substantially smaller compared to $\beta = 1, 2, 4$ cases shown in Fig. 1. However, a slow increase of σ_1 at very large times $t > 10^5$ is not excluded. We attribute this to a degeneracy of linear eigenmodes which, similar to the case of YMCA3 Hamiltonian (1), leads to a high fraction of chaotic phase space even for $\beta \to 0$, as discussed in Refs. 11 and 54 for three colors [we note that for Hamiltonian with two colors (1), there is no chaos in the limit of small β but only a significant energy exchange between two colors[11]]. Thus, a slow spreading at very large times for YMCA3 case may take place due to frequency degeneracy present for color fields initially located on a distance $R_C < \ell$. The effect of very slow Arnold diffusion[13,49] can also be present for a small fraction of global probability.

The interesting point is that the above exact frequency degeneracy is present only if initial color packets are close to each other. In the opposite case with their initial significant separation on a distance $R_C \gg \ell$, the effective nonlinear interactions between colors drop exponentially with R_C due to the localization of linear eigenmodes. In addition, the frequencies of eigenmodes populated for such packets with large separation $R_C \gg \ell$ and statistically different and have no exact degeneracy in contrast to the case with $R_C < \ell$. Thus, for $R_C \gg \ell$, we argue that this case corresponds to a very small effective interactions with $\beta_{eff} \propto \beta \exp(-2R_C/\ell) \ll 1$ and that the color YM fields remain confined and localized. This is confirmed by the results shown in Figs. 7 and 8, where we compare the close and distant location of initial color packets. We have clear deconfinement and spreading for $R_C = 1$ (for $W = 8$, $\beta = 2$, and $R_c = 1$, the fit gives $\alpha = 0.30 \pm 0.02$ which smaller than the value at $W = 4$ in Table I). In contrast, for $R_C \gg \ell$, there is confinement and localization of YM color fields. The increase of disorder strength from $W = 4$ in Fig. 7 to $W = 8$ in Fig. 8 gives at $R_C = 250$ a strong enhancement of localization of color YM fields. For distant initial

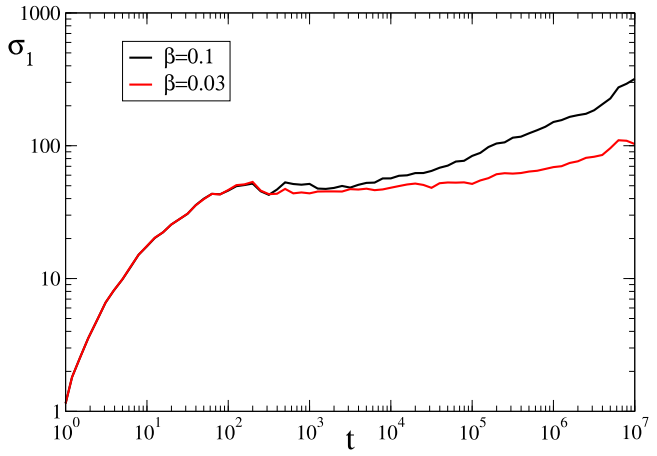

FIG. 6. Time evolution of the second moment σ_1 of the probability distribution defined in the text for the YMCA3 model with three colors for $\beta = 0.1$ (black curve) and $\beta = 0.03$ (red curve) at $W = 4$. At the initial time, the three color packets are located at three different sites $n = -1, 0, 1$. The results are shown for ten disorder realizations and logarithmic equidistant intervals of time.

positions of color fields $R_C = 250$, the second moment $\sigma_1(t)$ shows absolutely no growth with time as it is shown in Fig. 9.

It is interesting to note that the situation with localization–delocalization of color YM fields reminds those of a quantum problem of two interacting particles coherently propagating in a disorder potential and being localized if separated by a distance being larger than a one-particle localization length (see, e.g., Refs. 55–57).

C. Simple estimates for spreading exponent of YM colors

Here, we present simple estimates for the spreading exponent α of the second moment growth $\sigma_{1,2} \propto t^{\alpha}$. Following the approach described in Refs. 28 and 35, it is useful to rewrite Eq. (4) on the basis of eigenstates of the linear system at $\beta = 0$. The transformation from lattice representation to eigenstate basis reads $\psi_n^{\mu} = \sum_m Q_{nm}^{\mu} C_m^{\mu}$ for each color μ. Then, the time evolution Eq. (4) takes the form

$$i\frac{\partial C_m^{\mu}}{\partial t} = \varepsilon_m C_m^{\mu} + \beta \sum_{\mu' \neq \mu} \sum_{m_1 m_2 m_3} U_{mm_1 m_2 m_3}^{\mu'} C_{m_1}^{\mu} C_{m_2}^{\mu' *} C_{m_3}^{\mu'}, \qquad (5)$$

where ε_m are the eigenenergies of a linear system, which is the same for all colors. The transitions between linear eigenmodes take place only due to the nonlinear β-term with the transition matrix elements $U_{mm_1 m_2 m_3}^{\mu'} = \sum_n (Q_{nm}^{\mu})^{-1} Q_{nm_1}^{\mu'} (Q_{nm_2}^{\mu'})^* Q_{nm_3}^{\mu}$. Due to the exponential localization of linear eigenstates, the sum over each m-index in (5) contains about ℓ terms.

In Ref. 28, it was argued that with an assumption that there is a plateau of size Δn with random coefficients of approximately equal amplitudes and random signs or phases and zero amplitudes outside the plateau. Then, the population of states outside of plateau should go with the rate $\Gamma \sim |C|^6 \sim 1/(\Delta n)^3$ on nearby sites on a distance ℓ. This gives a diffusion rate $D \sim \ell^2 \Gamma \sim \ell^2/(\Delta n)^3 \sim (\Delta n)^2/t$

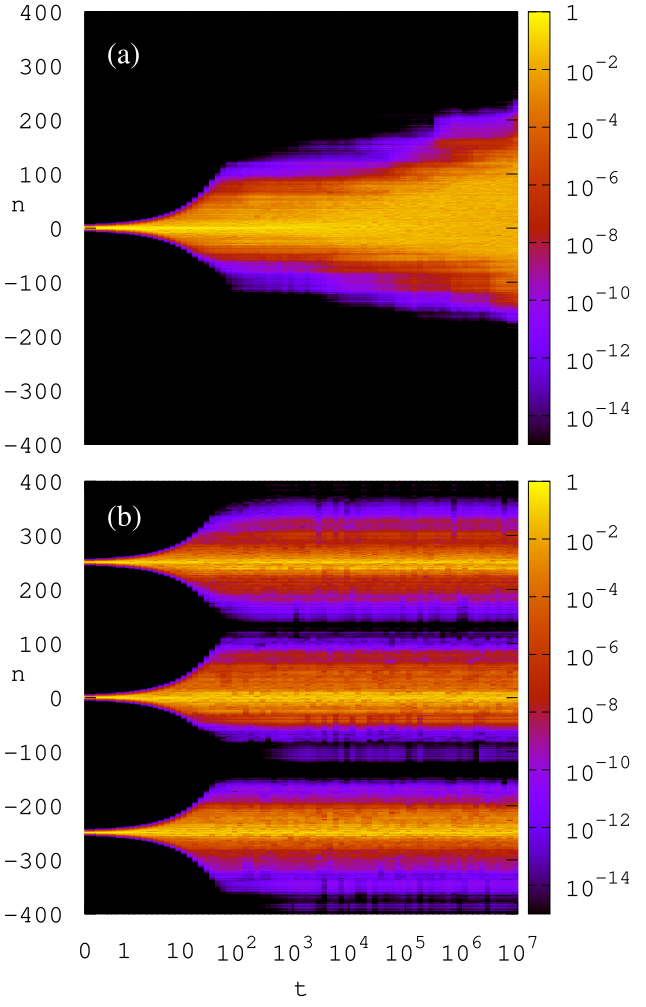

FIG. 7. Probability distribution as a function of time t for the YMCA3 model at $\beta = 2$ and $W = 4$; initial positions of three colors are $n = -1, 0, 1$ with $R_C = 1$ (a); $n = -250, 0, 250$ with $R_C = 250$ (b) for one disorder realization; the color bar shows probability $w(n)$ of YM color fields.

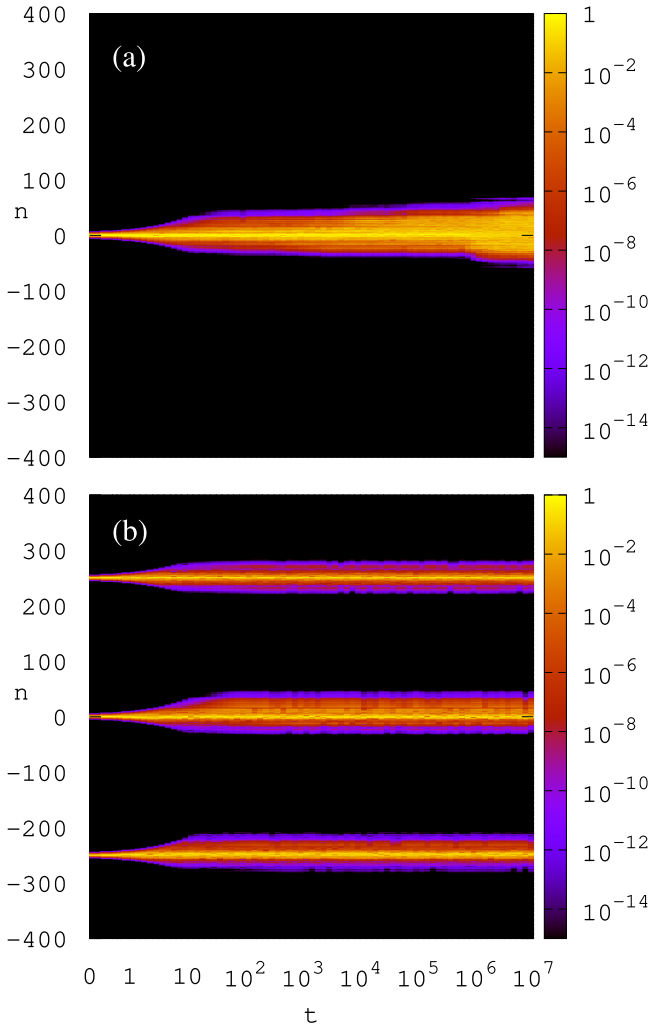

FIG. 8. Same as in Fig. 7 but for $W = 8$.

leading to the growth $(\Delta n)^2 \sim \sigma_{1,2} \sim t^\alpha$ with the spreading exponent $\alpha = 2/5$.

There are also other types of arguments leading to the same exponent $\alpha = 2/5$. In fact, the time evolution of (5) represents the nonlinear field dynamics involving many random frequency components describing a continuous chaotic flow. The spreading Δn in time is very slow and its Lyapunov exponent λ at given Δn is given by the nonlinear frequency $\lambda \sim \delta\omega \sim \beta/\Delta n$.[28,35] It is well established that for such a continuous chaotic flows with many frequency components, the diffusion rate D is related to the Lyapunov exponent λ, or typical nonlinear frequency $\delta\omega$, by the relation established in Refs. 58 and 59: $D \sim \lambda^3 \sim (\delta\omega)^3$. This relation was well confirmed for the Chirikov typical map which represents a generic model of such continuous chaotic flows[60] (see also recent work[61]). Since for (5) we have $\delta\omega \sim \beta/\Delta n$, this gives us $D \propto 1/(\Delta n)^3 \propto (\Delta n)^2/t$ and thus the spreading exponent is $\alpha = 2/5$, which is in agreement with the estimate given at Ref. 28. We note that for spreading in a disorder potential in higher dimension $d > 1$, this approach gives the spreading $(\Delta n)^2 = R^2 \sim t^\alpha$ with the exponent $\alpha = 2/(3d + 2)$ with $\alpha = 1/4$ for $d = 2$ (here, R is a 1D wavepacket size).[35]

Another estimate of α, proposed in Ref. 48, is based on the assumption that the transition rate is given by the Fermi golden rule as in linear equations of quantum mechanics. This gives $\Gamma \propto |C|^4 \sim 1/(\Delta n)^2$ and leads to $\alpha = 1/2$,

More complicated estimate arguments were pushed forward in Ref. 34 leading to the value $\alpha = 1/3$.

There are various physical arguments behind each of the estimate described above. However, the time evolution of nonlinear YM fields in the presence of a disorder is rather a complicated

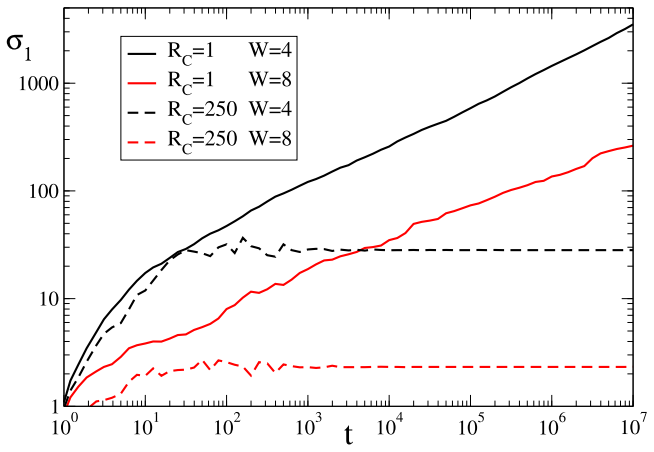

FIG. 9. Time dependence of $\sigma_1(t)$ for YMCA3 at $\beta = 2$ for the initial distance between color positions: $R_C = 1$ (full black curve for 20 disorder realizations at $W = 4$ same as in Fig. 1); $R_C = 250$ (dashed black curve for one disorder realization at $W = 4$ same as in Fig. 7); $R_C = 1$ (full red curve for 10 disorder realizations at $W = 8$); $R_C = 250$ (dashed red curve for one disorder realization at $W = 8$ same as in Fig. 8).

problem. The obtained numerical values of the spreading exponent are found to be approximately in the range of $0.3 \leq \alpha \leq 0.4$. Further numerical studies are required, with longer time evolution and larger number of disorder realizations, to determine more exactly the exponent value.

D. Dynamical thermalization

The studies of DANSE showed that in lattices of finite size, there is an emergence of dynamical thermalization with a thermal distribution of probabilities over linear eigenmodes.[53,62] This dynamical thermalization appears in DANSE only for nonlinearity $\beta > \beta_c$. We expect that this phenomenon will also take place for the YM models considered here. However, there is an important difference comparing to DANSE case: for YM models with a significant distance separation between color components, an effective nonlinearity becomes below the chaos border and thermalization is absent. We note that a thermalization in QCD is actively discussed in high energy physics (see, e.g., Ref. 63). However, here the dynamical origins of thermalization are never considered. Of course, the QCD is a purely quantum theory, in contrast to classical fields considered here, but the dynamical thermalization in finite quantum systems is now actively discussed in the field of quantum chaos and it is shown that at weak interactions between quantum fields, there is no thermalization (see, e.g., Ref. 64, and references therein). Thus, we expect that the concepts of classical and quantum chaos can highlight interesting research directions also for QCD as it happened to be the case for the SYK model of quantum gravity (see Ref. 64).

E. YM color breathers?

The mathematical proof given in Ref. 65 guarantees that nonlinear classical Hamiltonian lattices have generic solutions called discrete breathers. They represent time-periodic nonlinear fields localized, usually exponential, in space. Such breathers find a variety of applications as discussed in Ref. 66. It was shown that breathers exist also for the DANSE model with and without disorder.[67,68] Usually the breathers appear at a strong nonlinearity of self-interacting field that effectively creates a solution similar to an impurity energy level outside of the energy band in quantum mechanics. For the YM color fields (4), nonlinearity appears only due to interactions of different colors. We suppose that the breather solutions still can exist for the YM color dynamics on a discrete lattice. However, the verification of this conjecture requires further studies that are outside of the scope of this work.

IV. DISCUSSION

The dynamics of classical homogeneous Yang–Mills color fields and their chaotic properties have been investigated and well understood about two decades ago (see, e.g., Refs. 8–11). Here, we analyzed the spacial aspects of classical YM color fields and properties of their propagation in disorder potential in 1D. In the absence of interactions of YM fields, the color wavepackets are confined and exponentially localized by disorder similar to the Anderson localization of electron transport induced by disorder.[24–27] The interactions of YM fields lead to the deconfinement of colors, which, above a certain interaction threshold, spreads subdiffusively over the whole disordered lattice. The exponent of this algebraic spreading is found to be approximately in the range of $0.3 < \alpha < 0.4$, which is similar to the value found for the DANSE model[28,30,34] and observed in experiments on cold atoms Bose–Einstein condensate spreading in a disordered optical lattices.[43] Compared to the DANSE model, we show that YM color fields can be deconfined and delocalized only when the color components remain close to each other. In contrast, separated color wavepackets remain confined and localized by the disorder. Of course, the QCD theory is a theory of purely quantum fields, whereas here we studied dynamics of classical nonlinear fields. However, we expect that the obtained results for classical YM color field dynamics in a disorder potential will also be useful for solving the problem of YM fields deconfinement in the full quantum problem.

ACKNOWLEDGMENTS

This research has been partially supported through Grant NANOX No. ANR-17-EURE-0009 (Project MTDINA) in the frame of the *Programme des Investissements d'Avenir, France*.

DATA AVAILABILITY

The data that support the findings of this study are available within the article.

REFERENCES

[1] C. N. Yang and R. L. Mills, "Conservation of isotopic spin and isotopic gauge invariance," Phys. Rev. **96**, 191 (1954).
[2] A. M. Polyakov, "Particle spectrum in quantum field theory," Pis'ma Zh. Eksp. Teor. Fiz. **20**, 430 (1974) [JETP Lett. **20**, 194 (1974)].
[3] A. M. Polyakov, "Isomeric states of quantum fields," Zh. Eksp. Teor. Fiz. **68**, 1975 (1975) [Sov. Phys. JETP **41**(6), 988 (1976)].

[4]A. M. Polyakov, "Compact gauge fields and the infrared catastrophe," Phys. Lett. B **59**, 82 (1975).
[5]A. A. Belavin, A. M. Polyakov, A. S. Schwartz, and Y. S. Tyupkin, "Pseudoparticle solutions of the Yang-Mills equations," Phys. Lett. B **59**, 85 (1975).
[6]A. I. Vainstein, V. I. Zakharov, V. A. Novikov, and M. A. Shifman, "ABC of instantons," Sov. Phys. Usp. **25**, 195 (1982).
[7]D. M. Ostrovsky, G. W. Carter, and E. V. Shuryak, "Forced tunneling and turning state explosion in pure Yang-Mills theory," Phys. Rev. D **66**, 036004 (2002).
[8]S. G. Matinyan, G. K. Savvidi, and N. G. Ter-Arutunyan-Savvidi, "Classical Yang-Mills mechanics. Nonlinear color oscillations," Zh. Eksp. Teor. Fiz. **80**, 830 (1981) [Sov. Phys. JETP **53**(3), 421 (1981)].
[9]B. V. Chirikov and D. L. Shepelyanskii, "Stochastic oscillations of classical Yang-Mills fields," Pis'ma Zh. Eksp. Teor. Fiz. **34**(4), 171 (1981) [JETP Lett. **34**, 163 (1981)].
[10]S. G. Matinyan, G. K. Savvidi, and N. G. Ter-Arutyunyan-Savvidi, "Stochasticity of classical Yang-Mills mechanics and its elimination by using the Higgs mechanism," Pis'ma Zh. Eksp. Teor. Fiz. **34**(11) 613 (1981) [JETP Lett. **34**, 590 (1981)].
[11]B. V. Chirikov and D. L. Shepelyanskii, "Dynamics of some homogeneous models of classical Yang-Mills fields," Yad. Fiz. **36**, 1563 (1982) [Sov. J. Nucl. Phys. **36**(6), 908 (1982)].
[12]T. S. Biro, S. G. Matinyan, and B. Muller, *Chaos and Gauge Field Theory* (World Scientific Publishing, Singapore, 1994).
[13]B. V. Chirikov, "A universal instability of many-dimensional oscillator systems," Phys. Rep. **52**, 263 (1979).
[14]A. Lichtenberg and M. Lieberman, *Regular and Chaotic Dynamics* (Springer, New York, 1992).
[15]V. Arnold and A. Avez, *Ergodic Problems in Classical Mechanics* (Benjamin, New York, 1968).
[16]I. P. Cornfeld, S. V. Fomin, and Y. G. Sinai, *Ergodic Theory* (Springer-Verlag, New York, 1982).
[17]D. Berenstein and D. Kawai, "Smallest matrix black hole model in the classical limit," Phys. Rev. D **95**, 106004 (2017).
[18]T. Akutagawa, K. Hashimoto, T. Sasaki, and R. Watanabe, "Out-of-time-order correlator in coupled harmonic oscillators," J. High Energ. Phys. **2020**, 13 (2020).
[19]G. Savvidy, "Maximally chaotic dynamical systems," Ann. Phys. **421**, 168274 (2020).
[20]E. V. Shuryak, "Quantum chromodynamics and the theory of superdense matter," Phys. Rep. **61**, 71 (1980).
[21]P. Olesen, "Confinement and random fluxes," Nucl. Phys. B **200**(FS4), 381 (1982).
[22]S. M. Apenko, D. A. Kirzhnits, and Y. E. Lozovik, "Dynamical chaos, Anderson localization, and confinement," Pis'ma Zh. Eksp. Teor. Fiz. **36**(5), 172 (1982) [JETP Lett. **36**(5), 213 (1982)].
[23]E. V. Shuryak and J. J. M. Verbaarschot, "Random matrix theory and spectral sum rules for the Dirac operator in QCD," Nucl. Phys. A **560**, 306 (1993).
[24]P. W. Anderson, "Absence of diffusion in certain random lattices," Phys. Rev. **109**, 1492 (1958).
[25]Y. Imry, *Introduction to Mesoscopic Physics* (Oxford University Press, Oxford, 2002).
[26]E. Akkermans and G. Montambaux, *Mesoscopic Physics of Electrons and Photons* (Cambridge University Press, Cambridge, 2007).
[27]F. Evers and A. D. Mirlin, "Anderson transitions," Rev. Mod. Phys. **80**, 1355 (2008).
[28]D. L. Shepelyansky, "Delocalization of quantum chaos by weak nonlinearity," Phys. Rev. Lett. **70**, 1787 (1993).
[29]M. I. Molina, "Transport of localized and extended excitations in a nonlinear Anderson model," Phys. Rev. B **58**, 12547 (1998).
[30]A. S. Pikovsky and D. L. Shepelyansky, "Destruction of Anderson localization by a weak nonlinearity," Phys. Rev. Lett. **100**, 094101 (2008).
[31]C. Skokos, D. O. Krimer, S. Komineas, and S. Flach, "Delocalization of wave packets in disordered nonlinear chains," Phys. Rev. E **79**, 056211 (2009).
[32]S. Flach, D. O. Krimer, and C. Skokos, "Universal spreading of wave packets in disordered nonlinear systems," Phys. Rev. Lett. **102**, 209903 (2009).
[33]M. Mulansky and A. Pikovsky, "Energy spreading in strongly nonlinear disordered lattices," New J. Phys. **15**, 053015 (2013).
[34]T. V. Lapteva, M. I. Ivanchenko, and S. Flach, "Nonlinear lattice waves in heterogeneous media," J. Phys. A: Math. Theor. **47**, 493001 (2014).
[35]I. Garcia-Mata and D. L. Shepelyansky, "Delocalization induced by nonlinearity in systems with disorder," Phys. Rev. E **79**, 026205 (2009).
[36]C. Skokos and S. Flach, "Spreading of wave packets in disordered systems with tunable nonlinearity," Phys. Rev. E **82**, 016208 (2010).
[37]L. Ermann and D. L. Shepelyansky, "Destruction of Anderson localization by nonlinearity in kicked rotator at different effective dimensions," J. Phys. A: Math. Theor. **47**, 335101 (2014).
[38]I. Vakulchyk, M. V. Fistul, and S. Flach, "Wave packet spreading with disordered nonlinear discrete-time quantum walks," Phys. Rev. Lett. **122**, 040501 (2019).
[39]B. Many Manda, B. Senyange, and C. Skokos, "Chaotic wave-packet spreading in two-dimensional disordered nonlinear lattices," Phys. Rev. E **101**, 032206 (2020).
[40]T. Schwartz, G. Bartal, S. Fishman, and M. Segev, "Transport and Anderson localization in disordered two-dimensional photonic lattices," Nature (London) **446**, 52 (2007).
[41]Y. Lahini, A. Avidan, F. Pozzi, M. Sorel, R. Morandotti, D. N. Christodoulides, and Y. Silberberg, "Anderson localization and nonlinearity in one-dimensional disordered photonic lattices," Phys. Rev. Lett. **100**, 013906 (2008).
[42]J. E. Lye, L. Fallani, M. Modugno, D. S. Wiersma, C. Fort, and M. Inguscio, "Bose-Einstein condensate in a random potential," Phys. Rev. Lett. **95**, 070401 (2005).
[43]E. Lucioni, B. Deissler, L. Tanzi, G. Roati, M. Zaccanti, M. Modugno, M. Larcher, F. Dalfovo, M. Inguscio, and G. Modugno, "Observation of subdiffusion in a disordered interacting system," Phys. Rev. Lett. **106**, 230403 (2011).
[44]P. Petreczky, "Lattice QCD at non-zero temperature," J. Phys. G: Nucl. Part. Phys. **39**, 093002 (2012).
[45]O. Philipsen, "The QCD equation of state from the lattice," Prog. Part. Nucl. Phys. **70**, 55 (2013).
[46]U. Reinosa, J. Serreau, M. Tissier, and N. Wchebor, "Deconfinement transition in SU(2) Yang-Mills theory: A two-loop study," Phys. Rev. D **91**, 045035 (2015).
[47]B. Kramer and A. MacKinnon, "Localization: Theory and experiment," Rep. Prog. Phys. **56**, 1469 (1993).
[48]D. Basko, "Kinetic theory of nonlinear diffusion in a weakly disordered nonlinear Schrödinger chain in the regime of homogeneous chaos," Phys. Rev. E **89**, 022921 (2014).
[49]B. V. Chirikov and V. V. Vecheslavov, "Arnold diffusion in large systems," Zh. Eksp. Teor. Fiz. **112**, 1132 (1997) [JETP **85**(3), 616 (1997)].
[50]S. Fishman, Y. Krivopalov, and A. Soffer, "On the problem of dynamical localization in the nonlinear Schrödinger equation with a random potential," J. Stat. Phys. **131**, 843 (2008).
[51]J. Bourgain and W.-M. Wang, "Quasi-periodic solutions of nonlinear random Schrödinger equations," J. Eur. Math. Soc. **10**, 1 (2008).
[52]G. P. Korchemsky, "Review of AdS/CFT integrability, chapter IV.4: Integrability in QCD and $N < 4$ SYM," Lett. Math. Phys. **99**, 425 (2012).
[53]L. Ermann and D. L. Shepelyansky, "Quantum Gibbs distribution from dynamical thermalization in classical nonlinear lattices," New J. Phys. **15**, 12304 (2013).
[54]M. Mulansky, K. Ahnert, A. Pikovsky, and D. L. Shepelyansky, "Strong and weak chaos in weakly nonintegrable many-body Hamiltonian systems," J. Stat. Phys. **145**, 1256 (2011).
[55]D. L. Shepelyansky, "Coherent propagation of two interacting particles in a random potential," Phys. Rev. Lett. **73**, 2607 (1994).
[56]Y. Imry, "Coherent propagation of two interacting particles in a random potential," Europhys. Lett. **30**(7), 405 (1995).
[57]K. M. Frahm, "Eigenfunction structure and scaling of two interacting particles in the one-dimensional Anderson model," Eur. Phys. J. B **89**, 115 (2016).
[58]B. V. Chirikov, "Research concerning the theory of nonlinear resonance and stochasticity," Preprint N 267 (Institute of Nuclear Physics, Novosibirsk, 1969) [CERN Trans. 71-40, Geneva, October (1971)].
[59]A. B. Rechester, M. N. Rosenbluth, and R. B. White, "Calculation of the Kolmogorov entropy for motion along a stochastic magnetic field," Phys. Rev. Lett. **42**, 1247 (1979).
[60]K. M. Frahm and D. L. Shepelyansky, "Diffusion and localization for the Chirikov typical map," Phys. Rev. E **80**, 016210 (2009).

[61] T. Goldfriend and J. Kurchan, "Quasi-integrable systems are slow to thermalize but may be good scramblers," Phys. Rev. E **102**, 022201 (2020).
[62] M. Mulansky, K. Ahnert, A. Pikovsky, and D. L. Shepelyansky, "Dynamical thermalization of disordered nonlinear lattices," Phys. Rev. E **80**, 056212 (2009).
[63] J. Berges, M. P. Heller, A. Mazeliauskas, and R. Venugopalan, "Thermalization in QCD: theoretical approaches, phenomenological applications, and interdisciplinary connections," arXiv:2005.12299[hep-th] (2020).
[64] K. M. Frahm and D. L. Shepelyansky, "Dynamical decoherence of a qubit coupled to a quantum dot or the SYK black hole," Eur. Phys. J. B **91**, 257 (2018).
[65] R. S. MacKay and S. Aubry, "Proof of existence of breathers for time-reversible or Hamiltonian networks of weakly coupled oscillators," Nonlinearity **7**, 1623 (1994).
[66] S. Flach and A. V. Gorbach, "Discrete breathers—Advances in theory and applications," Phys. Rep. **467**, 1 (2008).
[67] G. Kopidakis, S. Komineas, S. Flach, and S. Aubry, "Absence of wave packet diffusion in disordered nonlinear systems," Phys. Rev. Lett. **100**, 084103 (2008).
[68] S. Iubini and A. Politi, "Chaos and localization in the discrete nonlinear Schrödinger equation," arXiv:2103.11041[nlin.CD] (2021).